

Angular distribution of medium-induced QCD cascades

Jean-Paul Blaizot^a, Leonard Fister^a, Yacine Mehtar-Tani^a

^a*Institut de Physique Théorique, CEA Saclay, F-91191 Gif-sur-Yvette, France*

Abstract

We provide a complete description of the angular distribution of gluons in a medium-induced QCD cascade. We identify two components in the distribution, a soft component dominated by soft multiple scatterings, and a hard component dominated by a few hard scatterings. The typical angle that marks the boundary between these two components is determined analytically as a function of the energy of the observed gluon and the size of the medium. We construct the complete solution (beyond the diffusion approximation) in the regime where multiple branchings dominate the dynamics of the cascade in the form of a power series in the number of collisions with the medium particles. The coefficients of this expansions are related to the moments of the distribution in the diffusion approximation and are determined analytically. The angular distribution may be useful in phenomenological studies of jet shapes in heavy-ion collisions.

Keywords: Perturbative QCD, Heavy-Ion collisions, Jet-quenching

PACS numbers: 12.38.-t, 24.85.+p, 25.75.-q

1. Introduction

Jet measurements at the LHC represent a highlight of the heavy-ion program. High energy jets have the potential to probe the nature of the hot and dense matter produced in heavy ion collisions, the so-called quark-gluon plasma. The data reveal indeed that jets are strongly attenuated as they traverse a quark-gluon plasma, and a careful study of this attenuation can help pinning down various properties of the plasma, such as some of its transport coefficients. Particularly interesting for the present work is the detailed analysis of the missing energy observed in imbalanced dijet events [1, 2, 3, 4]. The reconstruction of the energy and angular distribution of jets particles around the dijet axis has been achieved, and evidence has been obtained that the missing energy in the away side jet is found in the form of soft particles radiated at very large angles from the direction of the jet.

On the theory side, there is a large dispersion in the predictions of the various jet-quenching models, which calls for a more complete, first principle, theory of jets in heavy-ion collisions. This paper reports on progress in this direction. The angular distribution that we determine may be a useful ingredient to be implemented in Monte Carlo event generators that are developed by several groups [5, 6, 7, 8]. The present work builds on the probabilistic equation that describes the in-medium QCD cascade, and which was derived recently [9]. It controls the evolution with the size of the medium, L , of the inclusive distribution of partons produced in the cascade as a function of the energy and the transverse momentum of the observed gluon. By solving this equation, we can determine the angular distribution of the energy that is radiated by the leading particle. This is the aim of the present work.

Email addresses: jean-paul.blaizot@cea.fr (Jean-Paul Blaizot), leonard.fister@cea.fr (Leonard Fister), yacine.mehtar-tani@cea.fr (Yacine Mehtar-Tani)

The first moment of the angular distribution (or equivalently of the transverse momentum distribution) was discussed recently [10, 11]. Three regimes can be identified as a function of the energy ω of the observed gluon: when $\omega \lesssim E$, with E the energy of the leading particle, we are measuring the original parton, whose transverse momentum is not altered by radiation and is determined solely by multiple scattering with the medium. The typical transverse momentum that it acquires is $\langle k_\perp^2 \rangle \sim \hat{q}L$, where \hat{q} is the so-called quenching parameter and corresponds to a diffusion coefficient in transverse momentum space. As we shall shortly see, \hat{q} determines not only the physics of transverse momentum broadening but also that of medium-induced parton branchings. The second regime is that for which the energy ω of the observed gluon is much smaller than E but larger than the characteristic scale $\omega_s = \alpha_s^2 \hat{q} L^2$, where α_s is the strong coupling constant, which marks the onset of branchings. This gluon is most likely radiated by the leading parton, and can be produced anywhere inside the medium. Its typical transverse momentum is $\langle k_\perp^2 \rangle \sim \hat{q}L/2$, where $L/2$ is the average time spent by the radiated gluon in the medium. Finally, in the multiple branching regime, $\langle k_\perp^2 \rangle \sim \hat{q}t_*(\omega)$, with t_* the typical time spent in the medium by the measured parton:

$$t_*(\omega) \sim \frac{1}{\alpha_s} \sqrt{\frac{\omega}{\hat{q}}}. \quad (1)$$

In this regime, the typical transverse momentum is independent of the size of the medium.

In addition to the three regimes that we have just discussed, the character of the angular (or transverse momentum) distribution changes depending on whether k_\perp is smaller or larger than the typical transverse momentum $\langle k_\perp^2 \rangle$ that we have identified for each of the energy regimes: for $k_\perp \ll \langle k_\perp^2 \rangle$ multiple elastic scatterings dominate the dynamics, in the opposite case, i.e., $k_\perp \gg \langle k_\perp^2 \rangle$, only a single scattering determines the transverse momentum distribution and the distribution drops as k_\perp^{-4} . We shall refer to these two parts of the angular distribution as to the soft and hard components, respectively. The pattern of the various regimes is illustrated in Fig. 1.

In this paper, we complete the analysis undertaken with the study of the first moment, and provide a complete description of the angular distribution. In section 2, we recall the basic equation that governs the evolution with the size of the medium of the inclusive distribution of gluons, as a function of the energy ω and the angle θ of the observed gluon. We discuss two limiting cases. In the first case, the transverse momentum is integrated out, leaving us with the equation for the energy distribution. The other case corresponds to freezing the branching processes, and therefore on momentum broadening, with the identification of two regimes, that of multiple soft scatterings and that of hard single scattering. In section 3, we construct the angular distribution in the three regimes of energies that are discussed above. The analytic calculation of the moments of the soft component of the distribution are presented in Appendix A.

2. The equation for the in-medium QCD cascade

We consider the cascade of radiated gluons that is generated by a high energy gluon¹, with energy E , that propagates through a quark-gluon plasma. We focus on the medium-induced radiation, as governed by the BDMPSZ mechanism [12, 13, 15], and ignore here effects due to vacuum radiation. In this approach, both gluon splitting and momentum broadening are controlled by a single parameter \hat{q} , called the jet-quenching parameter. Thus, for instance, the average transverse momentum acquired by a parton through its collisions with the plasma constituents is $\langle k_\perp^2 \rangle \sim \hat{q}L$, with L the length of the medium crossed by the parton. The BDMPSZ mechanism takes into account the Landau-Pomeranchuk-Migdal (LPM) effect and

¹The extension to the case of a high energy quark is straightforward

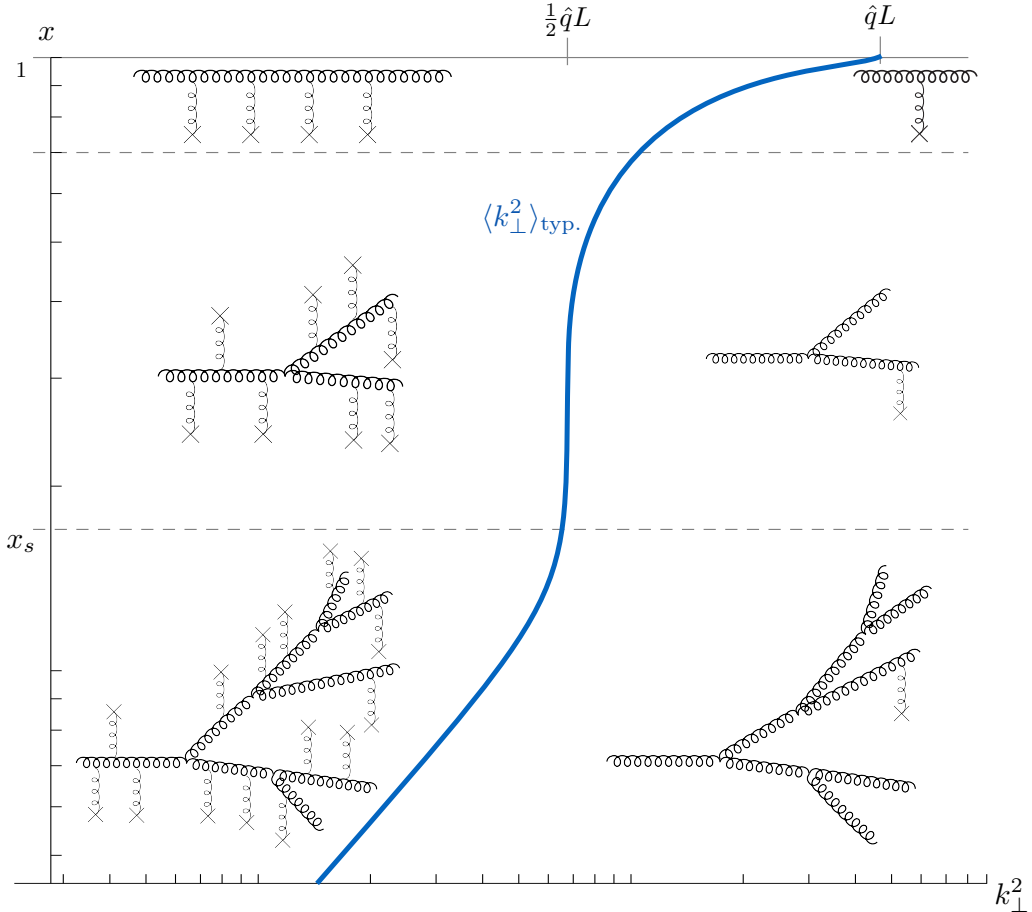


Figure 1: (Color online.) The various regimes of the physical processes (branching and scattering) that accompany the propagation of a fast parton in a dense medium. The thick (blue) line separates the regime of single hard, large angle, scattering, from that of soft, small angle, multiple scattering. Accordingly, the soft component of the angular distribution lies on the left of the blue line, the hard component on the right. The line $\omega/E \equiv x = x_s$ separates the region dominated by single branching from that of multiple branchings. The horizontal line below $x = 1$ indicates the region where the leading particle propagates without splitting, and merely suffers momentum broadening due to its collisions with the constituents of the medium.

provides the dominant contribution to the gluon spectrum for gluon frequencies $\omega_{\text{BH}} \lesssim \omega \lesssim \omega_c$, where $\omega_c \sim \hat{q}L^2$ is the maximum energy that can be taken away by a single gluon (the present analysis assumes² that $\omega_c \gtrsim E$). The lower limit is that of (Bethe-Heitler) incoherent emissions, and is reached when the branching time is of the order of the mean free path between successive collisions. The branching time for a gluon with energy ω is given by $\tau_{\text{br}}(\omega) \sim \sqrt{\omega/\hat{q}}$. It is associated with a transverse momentum scale $k_{\text{br}}(\omega) \sim (\omega\hat{q})^{1/4}$, and an emission angle $\theta_{\text{br}}(\omega) \sim (\hat{q}/\omega^3)^{1/4}$.

We are interested in the inclusive gluon distribution

$$D(x, \mathbf{k}, t) \equiv (2\pi)^2 x \frac{dN}{dx d^2\mathbf{k}}, \quad (2)$$

where $x = \omega/E$ is the energy fraction, and \mathbf{k} the transverse momentum, of the gluon observed at some time t along the cascade, with the maximum value of t equal to the length L of the

²We do not anticipate major qualitative changes when $\omega_c < E$ [16, 17].

medium. As was shown in [9], $D(x, \mathbf{k}, t)$ obeys the following integro-differential equation

$$\frac{\partial}{\partial t} D(x, \mathbf{k}, t) = \frac{1}{t_*} \int dz \mathcal{K}(z) \left[\frac{1}{z^2} \sqrt{\frac{z}{x}} D\left(\frac{x}{z}, \frac{\mathbf{k}}{z}, t\right) - \frac{z}{\sqrt{x}} D(x, \mathbf{k}, t) \right] + \int_{\mathbf{q}} \mathcal{C}(\mathbf{q}) D(x, \mathbf{k} - \mathbf{q}, t), \quad (3)$$

where we introduced in the last term a shorthand notation for the transverse momentum integrations: $\int_{\mathbf{q}} \equiv \int d^2 \mathbf{q} / (2\pi)^2$. This will be used throughout the paper. The kernel $\mathcal{K}(z)$ in the gain and loss terms (respectively the first and second term in the r.h.s. of Eq. (3)), can be written as [18]

$$\mathcal{K}(z) = \frac{[f(z)]^{5/2}}{[z(1-z)]^{3/2}}, \quad f(z) \equiv 1 - z + z^2. \quad (4)$$

It collects contributions from the z dependence of the actual branching time (left out in the definition³ of t_* , Eq. (5) below), and from the leading order splitting function $P_{gg}(z) = N_c [f(z)]^2 / z(1-z)$ where N_c is the number of colors (we restrict our discussion to purely gluonic cascades). Equation (3) combines two distinct physical effects: i) the branching of gluons, which preserves the angles but change the number of particles, and is described by the term proportional to $1/t_*$; ii) the momentum broadening due to collisions with the plasma constituents, which preserves the number of particles, and is described by the last term.

Two important approximations are involved in the derivation of Eq. (3). First, the typical duration of the branching process is assumed to be small compared to the total time spent by the gluon in the medium. This allows to treat the branchings as effectively instantaneous [18]. Second, the transverse momentum broadening that takes place during a branching is ignored (corrections involving the small transverse momentum induced during the splitting can be absorbed in corrections to \hat{q} [9, 19] (see also [20, 21] for related discussions of radiative corrections to p_\perp broadening). The branching is then treated as effectively collinear: After the splitting, the two new gluons carry fractions z and $1-z$ of both the initial energy and the initial transverse momentum. Thus when a gluon of energy ω_0 , and transverse momentum \mathbf{k}_0 splits into a gluon of energy ω_1 , and transverse momentum \mathbf{k}_1 and another gluon of energy ω_2 , and transverse momentum \mathbf{k}_2 , we have $\omega_1 = z\omega_0$, $\mathbf{k}_1 = z\mathbf{k}_0$ (and similarly for the other gluon, with $z \rightarrow 1-z$). It follows that $\theta_0 = k_0/\omega_0 = k_1/\omega_1 = \theta_1$, the angle is preserved in the splitting. On the other hand, if $z \ll 1$, $k_1 \ll k_0$, there is a degradation of the transverse momentum at each splitting along the cascade. The competition between this degradation of the transverse momentum that accompanies each splitting, with the accumulation of transverse momentum from collisions with the medium constituents, plays an important role in determining the form of the momentum distribution.

The quantity

$$\frac{1}{t_*} \equiv \frac{\bar{\alpha}}{\tau_{\text{br}}(E)} = \bar{\alpha} \sqrt{\frac{\hat{q}}{E}}, \quad (5)$$

with $\bar{\alpha} \equiv \alpha_s N_c / \pi$, is the basic rate of the branching processes. It depends on the energy E of the incoming parton, and on the medium through the jet-quenching parameter \hat{q} . We shall soon verify that t_* is the time at which most of the energy of the incoming parton has been radiated into soft gluons, and for this reason it is sometimes referred to as the stopping time. There are two basic control parameters in the problem: the energy E and the size L of the

³The actual branching time for offsprings carrying fractions z and $1-z$ of the initial energy is $\sqrt{z(1-z)}t_*$.

medium. We expect several regimes, depending on the values of these control parameters. The characteristic time t_* is related to the energy E as follows

$$E = \bar{\alpha}^2 \hat{q} t_*^2. \quad (6)$$

The frequency that characterizes the onset of the multiple branching regime is given by an analogous formula

$$\omega_s = \bar{\alpha}^2 \hat{q} L^2 = \bar{\alpha}^2 \omega_c, \quad (7)$$

where $\omega_c = \hat{q} L^2$. Gluons that are observed with an energy $\omega \lesssim \omega_s$ are likely to come from multiple branchings. Indeed the probability for emitting a gluon with energy ω in a distance L is $\bar{\alpha} L / \tau_{\text{br}}(\omega) = \bar{\alpha} L \sqrt{\hat{q} / \omega}$. This is of order unity when $\omega \sim \omega_s$ and larger when $\omega < \omega_s$. Now, by comparing the two equations above, we see that if $L > t_*$, then $\omega_s > E$ and one is always in the regime of multiple branching, since all radiated gluons have frequencies $\omega < E < \omega_s$. If on the other hand, $L < t_*$, the situation that we shall consider in this paper, then several regimes appear depending on whether we consider gluons with $\omega < \omega_s$ or $\omega > \omega_s$. These various regimes are illustrated in Fig. 1.

The last term in Eq. (3) describes momentum broadening, with the collision kernel given by

$$\mathcal{C}(\mathbf{q}) = w(\mathbf{q}) - (2\pi)^2 \delta(\mathbf{q}) \int_{\mathbf{q}'} w(\mathbf{q}'), \quad w(\mathbf{q}) = \frac{16\pi^2 \alpha_s^2 N_c n}{\mathbf{q}^4}, \quad (8)$$

where n is the density of scatterers (which we assume to be independent of t for simplicity). The quantity $w(\mathbf{q}) d^2 \mathbf{q} dt$ can be interpreted as the probability that the particle acquire a transverse momentum \mathbf{q} during dt : $w(\mathbf{q})$ is proportional to the elastic scattering cross section $d^2 \sigma_{\text{el}} / d^2 \mathbf{q}$ of the fast parton with the constituents of the medium, while $\mathcal{C}(\mathbf{q})$ is proportional to the so-called dipole cross section $\sigma(\mathbf{q})$, $\mathcal{C}(\mathbf{q}) = -N_c n \sigma(\mathbf{q}) / 2$. The jet-quenching parameter is related to the scattering rate. To logarithmic accuracy, it is given by

$$\hat{q}(\mathbf{p}^2) = \int_{\mathbf{q}} \mathbf{q}^2 w(\mathbf{q}) \simeq 4\pi \alpha_s^2 N_c n \ln \frac{\mathbf{p}^2}{m_D^2}, \quad (9)$$

where the Debye screening mass m_D regulates the singular behavior of the collision kernel at small momenta, while the upper cutoff is the typical momentum of the observed gluon. This formula makes sense, as does the definition of \hat{q} , only in the regime dominated by soft multiple scatterings. As we shall verify later this implies

$$\mathbf{p}^2 \lesssim \hat{q}(\mathbf{p}^2) L. \quad (10)$$

Insight into the general behavior of the solution of Eq. (3) can be gained by considering limiting cases where only branchings, or only scatterings take place. We start by the former case.

2.1. The energy distribution

By integrating Eq. (3) over the transverse momentum, one obtains an evolution equation for the energy density $D(x, t)$:

$$\frac{\partial}{\partial t} D(x, t) = \frac{1}{t_*} \int dz \mathcal{K}(z) \left[\sqrt{\frac{z}{x}} D\left(\frac{x}{z}, t\right) - \frac{z}{\sqrt{x}} D(x, t) \right]. \quad (11)$$

The scattering term vanishes upon integration over \mathbf{k} . Note that the function $D(x, t)$ has support only for $0 \leq x \leq 1$, which limits the first z -integral in Eq. (11) to $x < z < 1$. Note also that the potential endpoint singularities at $z = 1$ in the gain and loss terms cancel.

This equation can be solved exactly in the case where, in the kernel $\mathcal{K}(z)$ in Eq. (4), $f(z)$ is set equal to unity [22]. This simplification preserves the singular behavior of the kernel near $z = 0$ and $z = 1$, which determines the qualitative features of the solution. We shall use this exact solution from now on. For the initial condition $D(x, t = 0) = \delta(1 - x)$, this solution reads

$$D(x, t) = \frac{\tau}{\sqrt{x}(1-x)^{3/2}} \exp\left(-\pi \frac{\tau^2}{1-x}\right), \quad \tau \equiv \frac{t}{t_*}. \quad (12)$$

The essential singularity at $x = 1$ can be understood as a Sudakov suppression factor [15] (i.e. the vanishing of the probability to emit no gluon in any finite time). One can easily verify on this explicit solution the interpretation of t_* as a stopping time: after a time $t \simeq t_*$ most ($\gtrsim 98\%$) of the energy is to be found in the form of radiated soft ($x \lesssim 0.1$) gluons. Aside from this exponential factor, the solution has another remarkable property: for $x \ll 1$, $D(x, t)$ factorizes into a function of time and a function of x

$$D(x, t) \sim \frac{1}{\sqrt{x}} \tau e^{-\pi \tau^2}, \quad (x \ll 1). \quad (13)$$

The fact that the spectrum keeps the same x -dependence when t keeps increasing reflects the fact that the energy flows to $x = 0$ without accumulating at any finite value of x , a property reminiscent of wave turbulence [22]. The complete, energy conserving, solution involves a contribution $\propto \delta(x)$ whose coefficient grows with time as $1 - e^{-\pi \tau^2}$. Note that the onset of the regime dominated by multiple branchings is not directly visible on the scaling spectrum (13): there is no change of behavior when $x \lesssim x_s = \omega_s/E$.

The short time behavior of the solution (12) will be useful in the foregoing discussion. This can be obtained iteratively by inserting in the right hand side of Eq. (12) the leading particle solution $D^{(0b)}(x, t) = \delta(1 - x)$, where the upper script (0b) refers to the solution with zero branching. Alternatively, one can just simply expand Eq. (11) for small τ , and obtain, for x not too close to 1, the solution corresponding to one branching,

$$D^{(1b)}(x, t) = \frac{\tau}{\sqrt{x}(1-x)^{3/2}} = \frac{t}{t_*} x \mathcal{K}(x). \quad (14)$$

The last equality indicates the relation of this approximate distribution with the BDMPSZ spectrum.

2.2. The transverse momentum distribution for a single particle

We turn now to the scattering term. We may formally isolate its effects by letting $t_* \rightarrow \infty$, thereby effectively switching off the contributions of the gluon branching. The resulting distribution can then be written as

$$D(x, \mathbf{p}, t) = \delta(1 - x) \mathcal{P}(\mathbf{p}, t), \quad (15)$$

with $\mathcal{P}(\mathbf{p}, t)$ the probability for the leading gluon to acquire a transverse momentum \mathbf{p} during its propagation through the plasma for a duration t . This quantity obeys the equation

$$\frac{\partial}{\partial t} \mathcal{P}(\mathbf{p}, t) = \int_{\mathbf{q}} \mathcal{C}(\mathbf{q}) \mathcal{P}(\mathbf{p} - \mathbf{q}, t), \quad (16)$$

with the collision kernel given by Eq. (8). The equation (16) can be solved, formally, by Fourier transform. Setting $\mathcal{C}(\mathbf{q}) = \int d^2 \mathbf{r} e^{i \mathbf{q} \cdot \mathbf{r}} \mathcal{C}(\mathbf{r})$, we get

$$\mathcal{P}(\mathbf{p}, L) = \int d^2 \mathbf{r} \exp \left[-i \mathbf{p} \cdot \mathbf{r} + \int_0^L dt \mathcal{C}(\mathbf{r}) \right]. \quad (17)$$

Although this integral cannot be calculated analytically, its main features can be easily obtained. For instance, one may expand the second exponential in powers of the dipole cross section and give the result an interpretation in terms of multiple scattering [23]. One may then identify two components in the distribution $\mathcal{P}(\mathbf{p}, L)$: a soft component dominated by multiple scattering, in which case the multiple scattering expansion cannot be truncated to a finite number of terms, and a hard tail populated by rare events with single hard scatterings, for which the leading term in the multiple scattering series is sufficient to obtain an accurate determination of \mathcal{P} .

In order to quantify the separation between these two regimes, it is useful to consider an approximate expression of the Fourier transform $\mathcal{C}(\mathbf{r})$:

$$\mathcal{C}(\mathbf{r}) = 16\pi^2 \alpha_s^2 N_c n \int_{\mathbf{q}} \frac{e^{i\mathbf{q}\cdot\mathbf{r}} - 1}{\mathbf{q}^4} \simeq -\pi \alpha_s^2 N_c n \mathbf{r}^2 \ln \left(\frac{1}{\mathbf{r}^2 m_D^2} \right) = -\frac{1}{4} \hat{q}(\mathbf{r}^{-2}) \mathbf{r}^2, \quad (18)$$

where we have used the expression (9) for \hat{q} , and chosen $1/\mathbf{r}^2$ as the upper cut-off scale. Multiple scattering start to dominate when $L\mathcal{C}(\mathbf{r})$ in Eq. (17) becomes of order unity. We recover the condition (10) since in Eq. (17) $\mathbf{r}^{-1} \sim \mathbf{p}$.

In the regime dominated by multiple soft scatterings, the momentum transfer \mathbf{q} in a collision with medium particles is small compared to $\hat{q}L$, i.e., $m_D^2 \ll \hat{q}L$. Equivalently, in this regime, typically $\mathbf{q} \ll \mathbf{p}$ in Eq. (16), and one can transform this equation into a Fokker-Planck equation:

$$\frac{\partial}{\partial t} \mathcal{P}(\mathbf{p}, t) = \frac{1}{4} \left(\frac{\partial}{\partial \mathbf{p}} \right)^2 \left[\hat{q}(\mathbf{p}^2) \mathcal{P}(\mathbf{p}, t) \right], \quad (19)$$

with the jet quenching parameter $\hat{q}(\mathbf{p}^2)$ playing the role of a (momentum dependent) diffusion coefficient. It is given, to logarithmic accuracy, by Eq. (9). Hence, the typical transverse momentum squared acquired by a particle after a time t of propagation in the medium is $Q_s^2(t) = \hat{q}t$. In the approximation where one ignores the (logarithmic) dependence of \hat{q} on the dipole size \mathbf{r} , an approximation often referred to as the “harmonic approximation”, one can easily solve the diffusion equation (19). Assuming n , and hence \hat{q} , to be independent of t for simplicity, one gets

$$\mathcal{P}(\mathbf{p}, L) = \frac{4\pi}{Q_s^2(L)} \exp \left[-\frac{\mathbf{p}^2}{Q_s^2(L)} \right]. \quad (20)$$

As already emphasized, the diffusion picture is valid in the regime dominated by multiple scattering, and holds for $\mathbf{p}^2 \lesssim \hat{q}L$. Larger transverse momenta can be achieved through a single hard scattering. The expression for \mathcal{P} corresponding to a single hard scattering is easily obtained from Eq. (16), and reads

$$\mathcal{P}(\mathbf{p}, L) \approx (2\pi)^2 \delta(\mathbf{p}) \left[1 - L \int_{\mathbf{q}} w(\mathbf{q}) \right] + \frac{16\pi^2 \alpha_s^2 N_c n L}{\mathbf{q}^4}, \quad (21)$$

Note that because of this high momentum tail, the momentum distribution does not admit moments beyond the leading one (i.e., the integral of the distribution, related to conservation of probability, and the integral weighed by $|\mathbf{p}|$).

2.3. The evolution equation for the angular distribution

As we have mentioned, the splittings are treated as collinear, meaning that there is no deflection of particles caused by the splittings. It is then more convenient to follow the evolution of angles rather than that of the transverse momenta along the cascade. Accordingly we transform the transverse momentum distribution into an angular distribution, setting

$$D(x, \boldsymbol{\theta}) \equiv (2\pi)^2 x \frac{dN}{dx d^2\boldsymbol{\theta}}, \quad (22)$$

where

$$\boldsymbol{\theta} \equiv \frac{\mathbf{k}}{\omega} = \frac{\mathbf{k}}{xE}. \quad (23)$$

Note that $\boldsymbol{\theta}$ is a 2-dimensional vector collinear to \mathbf{k} , whose (small) magnitude equals the polar angle of the emitted gluon with respect to the initial direction of the leading particle. This distribution is normalized as follows

$$\int \frac{d^2\boldsymbol{\theta}}{(2\pi)^2} D(x, \boldsymbol{\theta}) = D(x). \quad (24)$$

In this new variable, Eq. (3) reads

$$\begin{aligned} \frac{\partial}{\partial t} D(x, \boldsymbol{\theta}, t) &= \frac{1}{t_*} \int dz \mathcal{K}(z) \left[\sqrt{\frac{z}{x}} D\left(\frac{x}{z}, \boldsymbol{\theta}, t\right) - \frac{z}{\sqrt{x}} D(x, \boldsymbol{\theta}, t) \right] \\ &+ \int \frac{d^2\boldsymbol{\theta}'}{(2\pi)^2} \mathcal{C}(\boldsymbol{\theta}', x) D(x, \boldsymbol{\theta} - \boldsymbol{\theta}', t), \end{aligned} \quad (25)$$

with (see Eq. (8))

$$\mathcal{C}(x, \boldsymbol{\theta}) = (xE)^2 \mathcal{C}(\mathbf{q}) = \frac{16\pi^2 \alpha_s^2 N_c n}{(xE)^2} \left[\frac{1}{\boldsymbol{\theta}^4} - \delta(\boldsymbol{\theta}) \int \frac{d^2\boldsymbol{\theta}'}{\boldsymbol{\theta}'^4} \right]. \quad (26)$$

The locality (in angle) of the splitting term reflects the collinearity of the splitting. In the diffusion approximation, i.e., $\boldsymbol{\theta}' \ll \boldsymbol{\theta}$ in Eq. (25), the equation (25) reduces to

$$\begin{aligned} \frac{\partial}{\partial t} D(x, \boldsymbol{\theta}, t) &= \frac{1}{t_*} \int dz \mathcal{K}(z) \left[\sqrt{\frac{z}{x}} D\left(\frac{x}{z}, \boldsymbol{\theta}, t\right) - \frac{z}{\sqrt{x}} D(x, \boldsymbol{\theta}, t) \right] \\ &+ \frac{1}{4(xE)^2} \left(\frac{\partial}{\partial \boldsymbol{\theta}} \right)^2 [\hat{q} D(x, \boldsymbol{\theta}, t)], \end{aligned} \quad (27)$$

with $\hat{q} \simeq 4\pi\alpha_s^2 N_c n \ln(\boldsymbol{\theta}^2/\boldsymbol{\theta}_D^2)$ and $\boldsymbol{\theta}_D \equiv m_D/\omega = m_D/(xE)$.

It useful to proceed in Fourier space. We set

$$D(x, \mathbf{u}, t) = \int \frac{d^2\boldsymbol{\theta}}{(2\pi)^2} D(x, \boldsymbol{\theta}, t) e^{-i\boldsymbol{\theta} \cdot \mathbf{u}}, \quad (28)$$

and get

$$\frac{\partial}{\partial t} D(x, \mathbf{u}, t) = \frac{1}{t_*} \int dz \mathcal{K}(z) \left[\sqrt{\frac{z}{x}} D\left(\frac{x}{z}, \mathbf{u}, t\right) - \frac{z}{\sqrt{x}} D(x, \mathbf{u}, t) \right] + \mathcal{C}(x, \mathbf{u}) D(x, \mathbf{u}, t), \quad (29)$$

where

$$\mathcal{C}(x, \mathbf{u}) = \int \frac{d^2\boldsymbol{\theta}}{(2\pi)^2} \mathcal{C}(x, \boldsymbol{\theta}) e^{-i\boldsymbol{\theta} \cdot \mathbf{u}}. \quad (30)$$

This equation is the same as that, Eq. (11), satisfied by $D(x, t)$, except for the last term which plays here the role of source term. We can then write the solution as follows

$$D(x, \mathbf{u}, L) = \int_0^L dt \int_x^1 \frac{dy}{y} D\left(\frac{x}{y}, \frac{L-t}{\sqrt{y}}\right) \mathcal{C}(y, \mathbf{u}) D(y, \mathbf{u}, t). \quad (31)$$

The function $D(x/y, (L-t)/\sqrt{y})$, given by the solution (12) of Eq. (11), plays here the role of a Green's function (and will be often referred to as such in the foregoing discussion). In Eq. (31) it takes the explicit form

$$D\left(\frac{x}{y}, \frac{L-t}{\sqrt{y}}\right) = \frac{L-t}{t_*\sqrt{x}\left(1-\frac{x}{y}\right)^{3/2}} \exp\left[-\frac{\pi}{y-x}\left(\frac{L-t}{t_*}\right)^2\right]. \quad (32)$$

We can easily verify the following convolution property

$$\int_x^1 \frac{dy}{y} D\left(\frac{x}{y}, \frac{L-t}{\sqrt{y}}\right) D(y, t) = D(x, L). \quad (33)$$

In the foregoing discussion we shall need this Green's function in various regimes. For $L-t \ll t_*$, it is simply the delta function $y\delta(y-x)$, corresponding to the propagation without any branching. For one branching, $D\left(\frac{x}{y}, \frac{L-t}{\sqrt{y}}\right)$ can be approximated by the solution (14). Finally, in the multiple scattering regime, the following integral will be useful

$$\int_0^\infty dt' D\left(\frac{x}{y}, \frac{t'}{\sqrt{y}}\right) = \frac{\sqrt{y}t_*}{2\pi\sqrt{x/y}\sqrt{1-x/y}}. \quad (34)$$

3. Determining the angular distribution of gluons

Solving Eq. (25) exactly is difficult. In this section, we shall obtain an analytic representation of the solution in the various regimes indicated in Fig. 1, where appropriate approximations can be made: $x \simeq 1$ which corresponds to the leading particle; $x_s \ll x \ll 1$ which corresponds to the primary gluon radiation, and finally the regime $x \ll x_s$ dominated by multiple branching. Part of the difficulty in solving Eq. (25) comes from the fact that, as we have already emphasized, the angular distribution has two distinct components: a hard component, corresponding to large angles produced by single hard scatterings, and a soft component that can be obtained as the solution of the diffusion equation (27). Besides, these two components are strongly modified by gluon branching.

The soft component admits moments, which is not the case for the hard component. The characteristic angle that marks the boundary between the soft and the hard components depends on x , i.e., on the amount of branching. It can be estimated by calculating the mean squared angle of the soft component, and we proceed to its determination in the next subsection.

3.1. The mean squared angle $\langle\theta^2\rangle$

We define the typical angle squared

$$\langle\theta^2\rangle = \frac{M_1(x, L)}{D(x, L)}, \quad (35)$$

where $M_1(x, L)$ is the first moment of the angular distribution obtained in the diffusion approximation, Eq. (27),

$$M_1(x, L) = \int \frac{d^2\theta}{(2\pi)^2} \theta^2 D(x, \theta, L). \quad (36)$$

This moment obeys the following equation [10]

$$\frac{\partial}{\partial t} M_1(x, t) = \frac{1}{t_*} \int dz \mathcal{K}(z) \left[\sqrt{\frac{z}{x}} M_1\left(\frac{x}{z}, t\right) - \frac{z}{\sqrt{x}} M_1(x, t) \right] + \frac{N^2 \hat{q}}{(xE)^2} D(x, t). \quad (37)$$

It can be solved formally by multiplying it by the Green's function (32) and integrating over t and y . We then obtain the following integral representation for $\langle \theta^2 \rangle$

$$\langle \theta^2 \rangle = \frac{\hat{q}}{E^2} \int_0^L dt \int_x^1 \frac{dy}{y^3} D\left(\frac{x}{y}, \frac{L-t}{\sqrt{y}}\right) \frac{D(y, t)}{D(x, L)}. \quad (38)$$

We now proceed to the approximations that are valid in the different regimes of interest.

When $x \simeq 1$, we can write

$$\int_x^1 \frac{dy}{y^3} D\left(\frac{x}{y}, \frac{L-t}{\sqrt{y}}\right) D(y, t) \simeq \int_x^1 \frac{dy}{y} D\left(\frac{x}{y}, \frac{L-t}{\sqrt{y}}\right) D(y, t) = D(x, L), \quad (39)$$

where we have used, in the first equality, that $y^3 \simeq y$ in the integral measure, and the property (33) in the last equality. We then get the simple result, which corresponds to the momentum broadening of the leading particle,

$$\langle \theta^2 \rangle = \frac{\hat{q}L}{E^2} = \theta_s^2(1, L), \quad \theta_s^2(x, L) \equiv \frac{\hat{q}L}{\omega^2} = \frac{\hat{q}L}{x^2 E^2}. \quad (40)$$

Let us turn now to the regime of primary gluon radiation, i.e., $x_s \ll x \ll 1$. It is easily verified that, when $x \ll 1$, the dominant contribution to $M_1(x, t)$ is obtained when the first D in Eq. (38) is $D^{(0b)}$ and the second one $D^{(1b)}$. That is, the dominant contribution corresponds to that of the momentum broadening of the radiated gluon from the time of its emission. The other contribution, corresponding to the momentum broadening of the leading particle before the splitting, is suppressed by a factor x^2 . We get then, keeping the two contributions,

$$\langle \theta^2 \rangle = \left(1 + \frac{1}{x^2}\right) \frac{\hat{q}L}{2E^2} = \frac{1}{2} (1 + x^2) \theta_s^2(x, L). \quad (41)$$

Let us now discuss the third regime, $x \ll x_s$, which is characterized by the multiple branchings. In the small x region, namely for $x \ll x_s$ multiple branchings require a non perturbative treatment. To do that we return to the expression (32) of the Green's function and note that the integral over y in Eq. (38) is weighed towards values $x \lesssim y \ll 1$. The Green's function (32) decays exponentially as a function of its time argument, except in the region

$$L - t \lesssim \sqrt{y} t_* \ll \sqrt{x_s} t_* = L. \quad (42)$$

On the other hand, $D(y, t)$ decays over a time scale of order $t_* \gg L$. On that time scale the Green's function appears as a sharply peaked function of its time argument. In order to extract the leading behavior in this regime, we can thus set $t \sim L$ in $D(y, t)$ in Eq. (38), and integrate freely the Green's function over $t' = L - t$ from 0 to ∞ . By using Eq. (34), one gets then

$$\begin{aligned} M_1(x, \theta, L) &= \frac{\hat{q}}{E^2} \int_x^1 \frac{dy}{y} \frac{\sqrt{y} t_*}{2\pi \sqrt{x/y} \sqrt{1-x/y}} \frac{1}{y^2} D(y, L) \\ &\approx \frac{\hat{q}}{E^2} D(x, L) \int_x^1 \frac{dy}{2\pi y^3} \frac{\sqrt{y}}{\sqrt{1-x/y}} \\ &\approx \frac{\hat{q}}{(xE)^2} D(x, L) \frac{t_* \sqrt{x}}{4}, \end{aligned} \quad (43)$$

where in the second line, we have used $D(y, t) \approx \sqrt{x/y} D(x, t)$ valid in the scaling regime $x \lesssim y \ll 1$, and in the last one we have set the lower bound of the integration to zero and used

$$\int_0^1 du \frac{u}{\sqrt{u(1-u)}} = \frac{\pi}{2}. \quad (44)$$

Finally, we get

$$\langle \theta^2 \rangle = \frac{1}{4\bar{\alpha}} \left[\frac{\hat{q}}{(xE)^3} \right]^{1/2} \equiv \theta_*^2(x). \quad (45)$$

In summary, the boundary of the soft part of the angular distribution is given at large x by $\theta_s^2(x, L)$ which depends on the size L of the medium, and at small x by $\theta_*^2(x)$ which is independent of L . The line that separates the two components of the distribution in Fig. 1 reflects qualitatively this behavior.

3.2. The leading parton: $x \simeq 1$

Recall that we focus in this analysis on leading gluons that have sufficient energy to escape the medium without being completely absorbed. That is, we assume $t_* \gg L$. The distribution (12) exhibits then a peak near $x \sim 1$ that corresponds to the leading particle, and a radiation spectrum growing as $x^{-1/2}$ for small decreasing values of x . When $x \sim 1$, the distribution takes then the factorized form

$$D(x, \boldsymbol{\theta}, L) \simeq \mathcal{P}(\boldsymbol{\theta}, L) D(x, L), \quad (46)$$

where $D(x, L)$ is energy distribution given by Eq. (12) (for $x \lesssim 1$), and $\mathcal{P}(\boldsymbol{\theta}, L)$ solves the equation that derives from Eq. (16) after making the change of variables $\boldsymbol{\theta} = \mathbf{k}/(xE)$, namely,

$$\frac{\partial}{\partial t} \mathcal{P}(\boldsymbol{\theta}, t) = \int \frac{d^2 \boldsymbol{\theta}'}{(2\pi)^2} \mathcal{C}(x, \boldsymbol{\theta}') \mathcal{P}(\boldsymbol{\theta} - \boldsymbol{\theta}', t), \quad (47)$$

with the initial condition $\mathcal{P}(\boldsymbol{\theta}, 0) = \delta(\boldsymbol{\theta})$. The solution of this equation has essentially been given already in the previous section. In the regime of multiple scatterings, i.e., for $\theta^2 \lesssim \theta_s^2(L, x)$ it reads (see Eq. (20))

$$\mathcal{P}(\boldsymbol{\theta}, L) = \frac{4\pi}{\theta_s^2(x, L)} \exp \left[-\frac{\boldsymbol{\theta}^2}{\theta_s^2(x, L)} \right]. \quad (48)$$

In the opposite case, $\theta \gg \theta_s(x, L)$, a single hard scatterings dominates the distribution (cf. Eq. (21)) and we have (see Eq. (21))

$$\mathcal{P}(\boldsymbol{\theta}, L) = \frac{16\pi^2 \alpha_s^2 N_c n L}{(xE)^2 \boldsymbol{\theta}^4} \sim \frac{\theta_s^2(L, x)}{\boldsymbol{\theta}^4}. \quad (49)$$

3.3. Single BDMPSZ radiation: $x_s \ll x \ll 1$

Let us now discuss the angular distribution of the primary gluon emissions off the leading particle. In this regime the energy distribution is given by the leading order BDMPSZ distribution,

$$D(x, L) \simeq \frac{L}{t_* \sqrt{x}}, \quad (50)$$

and we expect also the angular distribution to be given by a single radiation that undergoes multiple scatterings. To see that, we look for the single branching contribution in Eq. (25),

$$\begin{aligned} \frac{\partial}{\partial t} D(x, \boldsymbol{\theta}, t) &= \frac{1}{t_*} \int dz \mathcal{K}(z) \left[\sqrt{\frac{z}{x}} D^{(0b)} \left(\frac{x}{z}, \boldsymbol{\theta}, t \right) - \frac{z}{\sqrt{x}} D^{(0b)}(x, \boldsymbol{\theta}, t) \right] \\ &+ \int \frac{d^2 \boldsymbol{\theta}'}{(2\pi)^2} \mathcal{C}(\boldsymbol{\theta}', x) D(x, \boldsymbol{\theta} - \boldsymbol{\theta}', t), \end{aligned} \quad (51)$$

where the zero branching contribution is given by

$$D^{(0b)}(x, \boldsymbol{\theta}, t) = \delta(1-x) \mathcal{P}(\boldsymbol{\theta}, t). \quad (52)$$

By performing the integration over z in Eq. (51), one gets

$$\frac{\partial}{\partial t} D(x, \boldsymbol{\theta}, t) = \frac{1}{t_*} x \mathcal{K}(x) \mathcal{P}(\boldsymbol{\theta}, t) + \int \frac{d^2 \boldsymbol{\theta}'}{(2\pi)^2} \mathcal{C}(\boldsymbol{\theta}', x) D(x, \boldsymbol{\theta} - \boldsymbol{\theta}', t). \quad (53)$$

By using the Green's function $\mathcal{P}(x, \boldsymbol{\theta}, t - t_0)$ that obeys the equation

$$\frac{\partial}{\partial t} \mathcal{P}(x, \boldsymbol{\theta}, t - t_0) - \int \frac{d^2 \boldsymbol{\theta}'}{(2\pi)^2} \mathcal{C}(\boldsymbol{\theta}', x) \mathcal{P}(x, \boldsymbol{\theta} - \boldsymbol{\theta}', t - t_0) = \delta(\boldsymbol{\theta}) \delta(t - t_0), \quad (54)$$

one obtains

$$D(x, \boldsymbol{\theta}, L) = \int_0^L \frac{dt}{t_*} \int \frac{d^2 \boldsymbol{\theta}'}{(2\pi)^2} \mathcal{P}(x, \boldsymbol{\theta} - \boldsymbol{\theta}', L - t) x \mathcal{K}(x) \mathcal{P}(\boldsymbol{\theta}', t). \quad (55)$$

Note that $\mathcal{P}(1, \boldsymbol{\theta}, t) \equiv \mathcal{P}(\boldsymbol{\theta}, t)$.

This equation can be understood as follows: the leading parton broadens from 0 to t with a probability $\mathcal{P}(\boldsymbol{\theta}', t)$, emits a soft gluon at time t , which propagates from t to L and whose distribution broadens according to $\mathcal{P}(x, \boldsymbol{\theta} - \boldsymbol{\theta}', L - t)$. For sufficiently small x , the angular deviation of the radiated gluon is larger than that of the leading parton. Accordingly one can neglect $\boldsymbol{\theta}'$ in the argument of the first \mathcal{P} , which allows us to perform trivially the integral over $\boldsymbol{\theta}'$,

$$\int \frac{d^2 \boldsymbol{\theta}'}{(2\pi)^2} \mathcal{P}(\boldsymbol{\theta}', t) = 1. \quad (56)$$

We finally get,

$$D(x, \boldsymbol{\theta}, L) \simeq \int_0^L \frac{dt}{t_*} \mathcal{P}(x, \boldsymbol{\theta}, L - t) x \mathcal{K}(x). \quad (57)$$

One can check that the moments of the angular distribution that are calculated in Appendix A using a different technique, coincide indeed with those of the distribution (57).

3.4. Multiple branchings: $x \ll x_s$

We are left now with the fully non-perturbative regime, i.e., $x \ll x_s$, where, in the soft region, both multiple scatterings and multiple branchings must be resummed. In order to solve Eq. (25) in this regime, we look for a solution as a power series in the number of scatterings. Our starting point is Eq. (31), which we rewrite here for convenience

$$D(x, \mathbf{u}, L) = \int_0^L dt \int_x^1 \frac{dy}{y} D\left(\frac{x}{y}, \frac{L-t}{\sqrt{y}}\right) \mathcal{C}(y, \mathbf{u}) D(y, \mathbf{u}, t). \quad (58)$$

This form of the equation allows us to resum easily the multiple scattering series. To that aim, we set

$$D(x, \mathbf{u}, t) = \sum_{n=0}^{\infty} D_n(x, \mathbf{u}, t), \quad (59)$$

with D_n of order \mathcal{C}^n . We obtain then, from Eq. (58),

$$D_n(x, \mathbf{u}, L) = \int_0^L dt \int_x^1 \frac{dy}{y} D\left(\frac{x}{y}, \frac{L-t}{\sqrt{y}}\right) \mathcal{C}(y, \mathbf{u}) D_{n-1}(y, \mathbf{u}, t), \quad (60)$$

with $D_0(x, \mathbf{u}, t) = D(x, t)$, and

$$\mathcal{C}(x, \mathbf{u}) = \int \int \frac{d^2 \boldsymbol{\theta}}{(2\pi)^2} \mathcal{C}(x, \boldsymbol{\theta}) e^{-i\boldsymbol{\theta} \cdot \mathbf{u}} \simeq -\frac{\pi \alpha_s^2 N_c n}{(xE)^2} \mathbf{u}^2 \ln \left(\frac{1}{\mathbf{u}^2 \theta_D^2} \right), \quad \theta_D \equiv \frac{m_D}{xE}. \quad (61)$$

To proceed we note that the dependence of $\mathcal{C}(y, \mathbf{u})$ on the variables y and \mathbf{u} occurs in the form

$$\mathcal{C}(y, \mathbf{u}) \sim \frac{\mathbf{u}^2}{y^2} \ln \left(\frac{y^2 E^2}{\mathbf{u}^2 m_D^2} \right), \quad (62)$$

so that

$$\frac{\mathcal{C}(y, \mathbf{u})}{\mathcal{C}(x, \mathbf{u})} = \frac{x^2 \ln \left(\frac{y^2 E^2}{\mathbf{u}^2 m_D^2} \right)}{y^2 \ln \left(\frac{x^2 E^2}{\mathbf{u}^2 m_D^2} \right)} = \frac{x^2}{y^2} \left[1 + \frac{\ln \left(\frac{y^2}{x^2} \right)}{\ln \left(\frac{x^2 E^2}{\mathbf{u}^2 m_D^2} \right)} \right]. \quad (63)$$

The logarithm in the denominator has typically a large argument: this is because in the multiple scattering regime, the typical angle $\theta \sim 1/u_\perp$ is achieved by multiple collisions deflecting the particle by an angle $\theta_D = m_D/(xE) \ll 1/u_\perp$. On the other hand, we have already observed that the integral over y in Eq. (60) is dominated by values of y larger but of the order of x . Therefore, the ratio of logarithms is generically small and can be neglected. Thus, in a first approximation, one can write

$$\mathcal{C}(y, \mathbf{u}) \simeq \mathcal{C}(x, \mathbf{u}) \frac{x^2}{y^2}. \quad (64)$$

This allows us to separate the variables in Eq. (60), which becomes then

$$D_n(x, \mathbf{u}, L) \simeq \mathcal{C}(x, \mathbf{u}) \int_0^L dt \int_x^1 \frac{dy}{y} D \left(\frac{x}{y}, \frac{L-t}{\sqrt{y}} \right) \frac{x^2}{y^2} D_{n-1}(y, \mathbf{u}, t). \quad (65)$$

The structure of this integral resembles that encountered when computing the mean transverse momentum squared, Eq. (38). We may then proceed similarly as in Eq. (43) in order to extract the leading behavior, and set $t \sim L$ in $D_{n-1}(y, \mathbf{u}, t)$ in Eq. (65), and integrate freely the Green's function over $t' = L - t$ from 0 to ∞ . Then, proceeding by recursion, we postulate the following form of the solution

$$D_n(x, \mathbf{u}, L) = c_n \left[\mathcal{C}(x, \mathbf{u}) t_*(x) \right]^n D(x, L), \quad (66)$$

where, for $x \ll x_s$, $D(x, L) \sim 1/\sqrt{x} f(L)$ and

$$t_*(x) = \frac{1}{4\bar{\alpha}} \sqrt{\frac{Ex}{\hat{q}}}, \quad (67)$$

The unknowns in Eq. (66) are the coefficients c_n . These are obtained by substituting the expression (66) in Eq. (60). We obtain then the recursion formula

$$c_n = c_{n-1} t_*^{-1}(x) \int_0^\infty dt' \int_0^1 \frac{dy}{y} D \left(\frac{x}{y}, \frac{t'}{\sqrt{y}} \right) \left(\frac{x}{y} \right)^{\frac{3n+1}{2}}, \quad (68)$$

or, using the explicit value of the integral (34)

$$c_n = c_{n-1} \frac{1}{2\pi} \int_0^1 du \frac{u^{\frac{3n-2}{2}}}{\sqrt{1-u}}. \quad (69)$$

The integration over u yields

$$\int_0^1 du \frac{u^{\frac{3n-2}{2}}}{\sqrt{1-u}} = B\left(\frac{3n}{2}, \frac{1}{2}\right) = \frac{\Gamma\left(\frac{3n}{2}\right)\Gamma\left(\frac{1}{2}\right)}{\Gamma\left(\frac{1+3n}{2}\right)}. \quad (70)$$

Recalling that $\Gamma(1/2) = \sqrt{\pi}$ and the fact that $c_0 = 1$, we finally get

$$c_n = \prod_{m=1}^n \frac{2}{\sqrt{\pi}} \frac{\Gamma\left(\frac{3m}{2}\right)}{\Gamma\left(\frac{1+3m}{2}\right)}. \quad (71)$$

These coefficients entirely determine the Fourier transform $D(x, \mathbf{u}, L)$ (see Eqs. (59) and (66)), from which the angular distribution $D(x, \theta, L)$ can in principle be deduced by performing the inverse Fourier transform. This can only be done numerically and remains a delicate procedure.

We have carried it in the harmonic approximation,

$$\mathcal{C}(x, \mathbf{u}) \approx \frac{1}{4} \frac{\hat{q}}{(xE)^2} \mathbf{u}^2, \quad (72)$$

where the logarithmic dependence of the dipole cross-section on \mathbf{u} and x is ignored. This approximation, which is equivalent to the diffusion approximation, does not allow us to explore the tail of the distribution for very large angles (see below), but it allows us to determine the distortion of the main peak. In this approximation, we simply get

$$D(x, \mathbf{u}, L) = D(x, L) \sum_{n=0}^{\infty} c_n \left[-\frac{1}{4} \theta_*^2(x) \mathbf{u}^2 \right]^n, \quad (73)$$

where we have used the fact that $\hat{q}_*(x) = (xE)^2 \theta_*^2(x)$. After performing an inverse Fourier transform we can write the angular distribution as follows,

$$D(x, \theta, L) = \frac{4\pi}{\theta_*^2(x)} \eta\left(\frac{\theta^2}{\theta_*^2(x)}\right) D(x, L), \quad (74)$$

where the scaling function η is given by

$$\eta\left(\frac{\theta^2}{\theta_*^2(x)}\right) = \frac{1}{4\pi} \theta_*^2(x) \int d^2\mathbf{u} e^{i\boldsymbol{\theta} \cdot \mathbf{u}} \sum_{n=0}^{\infty} c_n \left[-\frac{1}{4} \theta_*^2(x) \mathbf{u}^2 \right]^n. \quad (75)$$

After integrating over the azimuthal angle and renaming the variables, $z = \theta^2/\theta_*^2(x)$ and $2\alpha = |\mathbf{u}|\theta_*(x)$, we can rewrite Eq. (75) as

$$\eta(z) = \int_0^{\infty} d\alpha J_0(2\sqrt{z}\alpha) \sum_{n=0}^{\infty} c_n (-\alpha^2)^n, \quad (76)$$

where J_0 is a Bessel function. Note that the property (24) implies that

$$\int_0^{\infty} dz \eta(z) = 1. \quad (77)$$

In Fig. 2 we have plotted the angular distribution $\eta(z)$ in the multiple branching regime. For the numerical evaluation we have computed the first 500 terms in the series (73). We have checked firstly, that the first three moments of the distribution agree with the moments computed analytically from Eq. (A.17) and, secondly, that the large angle behavior matches the asymptotic limit, see Eq. (A.21). This limit also suggests a one-parameter fit of the full distribution, with the functional form

$$\eta_{\text{fit}}(z) = \frac{4c^{3/2}}{3\sqrt{\pi}} e^{-cz^{2/3}}, \quad (78)$$

where the normalisation is such that Eq. (77) is satisfied. For the fit-parameter we find $c \approx 1.68$. For comparison we have plotted the fit $\eta_{\text{fit}}(z)$ and also an exponential distribution $\eta_{\text{exp}}(z) = e^{-z}$ that has the first two moments identical to $\eta(z)$ in Fig. 2. The distributions have similar shapes, which comfort the choice of the exponential distribution in previous phenomenological studies of the missing energy in dijet events in Pb-Pb collisions [24, 10].

Consider finally the hard part of the distribution. The single scattering limit, achieved when $\theta \gg \theta_*(x)$ can be recovered by Fourier transforming the first term in the series, $D_1(x, \mathbf{u}, t)$. One can also obtain it right away from Eq. (31), which yields

$$D_1(x, \boldsymbol{\theta}, L) = \int_0^L dt \int \frac{dy}{y} D\left(\frac{x}{y}, \frac{L-t}{\sqrt{y}}\right) \frac{x^2}{y^2} \mathcal{C}(\boldsymbol{\theta}, y) D(y, t). \quad (79)$$

Calculating the integral (79) in the same way as we did for similar ones earlier, one easily obtains

$$D_1(x, \boldsymbol{\theta}, L) \approx D(x, L) \mathcal{C}(\boldsymbol{\theta}, x) \frac{t_* \sqrt{x}}{4} \approx D(x, L) \frac{\theta_*^2(x)}{\theta^4}, \quad \theta_*^2(x) = \frac{4\pi^2 \alpha_s^2 N_c n t_* \sqrt{x}}{x^2 E^2}. \quad (80)$$

We can write

$$\theta_*^2(x) \equiv \frac{1}{4\bar{\alpha}} \left[\frac{\hat{q}}{(xE)^3} \right]^{1/2} = \langle \theta^2 \rangle. \quad (81)$$

This is the typical angle squared of gluons in the multiple branching regime. The prefactor 1/4 is chosen to match the first moment, i.e., $\langle \theta^2 \rangle = \theta_*^2(x)$. Note that this angle $\theta_*(x)$ is independent of the size of the medium.

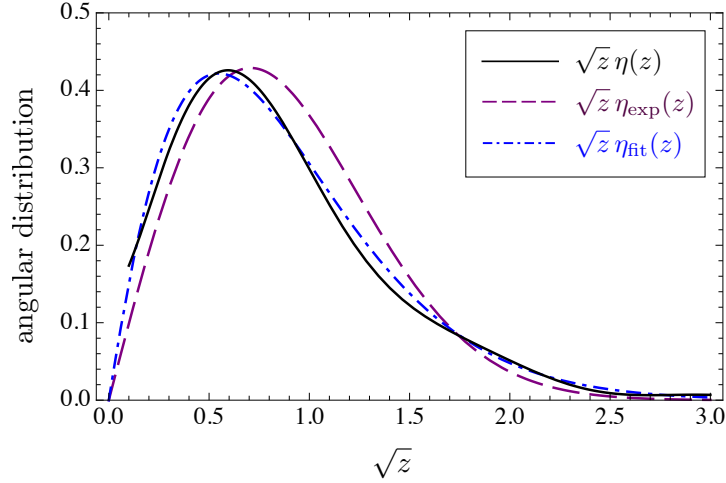


Figure 2: (Color online.) The angular distribution (76) of a gluon in the multiple branching regime (solid black line) compared to an exponential distribution with identical first two moments (dashed purple line). It can be fitted with a single parameter function (cf. Eq. (78)) inspired by the large angle limit (A.21) (dashed-dotted blue line).

4. Summary

In this work, we have constructed solutions to the equation that governs the evolution with the length of the medium of the inclusive gluon distribution along the medium-induced cascade

that is initiated by a hard gluon of energy E . This equation resums multiple branchings and scatterings, which are responsible for the multiplication of partons along the cascade and for their momentum broadening. We focused on the case where the energy of the leading particle is large enough so that it escapes the medium with a sizable fraction of its initial energy, that is, the stopping time t_* is larger than L , or equivalently $E \gg \omega_s = \bar{\alpha}^2 \hat{q} L^2$. This is the relevant condition to study the substructure of jets that are measured in Heavy-Ion collisions. In this case, one can identify three distinct regimes in the angular distribution, depending on the value of the energy ω of the energy of the observed gluon.

The first regime, which reflects the property of the leading particle, is characterized by an energy $\omega \lesssim E$. The corresponding distribution shows a slight broadening in energy (towards lower energies) and angles (towards larger angles) due to soft gluon emissions and elastic kicks, respectively. These two effects are here independent of one another, which translates into the factorisation of the energy and the angular distributions. The typical transverse momentum acquired by multiple scatterings in this regime is $\langle k_\perp^2 \rangle = \hat{q} L$, corresponding to the average angle squared $\langle \theta^2 \rangle = \hat{q} L / E^2$.

The second regime corresponds to gluons in the cascade that have been primarily radiated by the leading partons and are to be found in the energy range $\omega_s \ll \omega \ll E$. The energy distribution is given by the BDMPSZ spectrum. These gluons can be emitted anywhere inside the medium and their angular broadening is determined by brownian motion which yields, on average

$$\langle \theta^2 \rangle = \theta_s^2(\omega, L) = \frac{\hat{q} L}{\omega^2}. \quad (82)$$

In the regimes discussed so far, the angular distribution is determined by processes that involve at most one gluon splitting. When $\omega \ll \omega_s$, multiple branching occur with probability one. This is the third regime. We already made the remark that the onset of the multitude branching regime at $\omega = \omega_s$ is not visible in the energy distribution which exhibits a scaling behavior $\omega^{-1/2}$ for all $x \ll 1$. But the character of the angular distribution changes at $\omega \lesssim \omega_s$. Indeed, in this regime, the characteristic squared angle is given by

$$\theta_*^2(\omega) = \frac{\hat{q} t_*(\omega)}{\omega^2} = \frac{1}{\bar{\alpha}} \sqrt{\frac{\hat{q}}{\omega^3}}. \quad (83)$$

It is independent of the size of the medium: it corresponds to the momentum broadening of the observed gluon, during the time $t_*(\omega) \ll L$ that this gluon spends in the medium from the moment it has been emitted.

The characteristic times that have been recalled above, and which are related to average angle squared of the soft part of the angular distribution, mark the frontier between this soft part of the distribution dominated by soft multiple scatterings, and its hard tail dominated by hard scattering. This hard tail can be determined perturbatively at large angle by taking into account a single hard scattering. The full angular distribution can be constructed as a power series in the number of scatterings and computed numerically, as was shown in this paper.

These results provide a first principle determination of the angular distribution of the gluons radiated by a jet in a medium. They should be useful in future phenomenological studies of jet shapes.

Acknowledgements

We would like to thank F. Gelis for helpful discussions. LF acknowledges fruitful discussions with E. Iancu on related topics. This research is supported by the European Research Council under the Advanced Investigator Grant ERC-AD-267258.

Appendix A. Moments of the angular distribution in the diffusion approximation

In this Appendix, we extend the calculation presented in Sect. 3.1 to the calculation of all the moments of the soft component of the angular distribution, that is, of the solution of Eq. (27). We define normalized moments as follows

$$\langle \theta^{2N} \rangle = \frac{M_N(x, L)}{M_0(x, L)} = \frac{\int_{\theta} \theta^{2N} D(x, \theta, L)}{D(x, L)}, \quad (\text{A.1})$$

where $D(x, L) = \int_{\theta} D(x, \theta, L)$. To obtain the equation satisfied by $M_N(x, t)$, we multiply Eq. (27) by θ^{2N} , and integrate over θ . We obtain

$$\frac{\partial}{\partial t} M_N(x, t) = \frac{1}{t_*} \int dz \mathcal{K}(z) \left[\sqrt{\frac{z}{x}} M_N\left(\frac{x}{z}, t\right) - \frac{z}{\sqrt{x}} M_N(x, t) \right] + \frac{N^2 \hat{q}}{(xE)^2} M_{N-1}(x, t). \quad (\text{A.2})$$

The last term was obtained by integrating by parts over θ in order to eliminate the Laplacian, and using the fact that all moments vanish at large θ . Eq. (A.2) is an inhomogeneous equation for the moment of order N , where the moment order $N - 1$ plays the role of a source. This equation can be solved in the same way as Eq. (37), that is

$$M_N(x, L) = \frac{N^2 \hat{q}}{E^2} \int_0^L dt \int_x^1 \frac{dy}{y^3} D\left(\frac{x}{y}, \frac{L-t}{\sqrt{y}}\right) M_{N-1}(y, t), \quad (\text{A.3})$$

with $D(x/y, (L-t)/\sqrt{y})$ given explicitly in Eq. (32).

The ratios of moments, $r_N \equiv x^2 M_N / M_{N-1}$, obtained by solving numerically Eq. (A.2), are plotted in Fig. 2. The limiting behaviors agree perfectly with the analytical analysis that we now turn to.

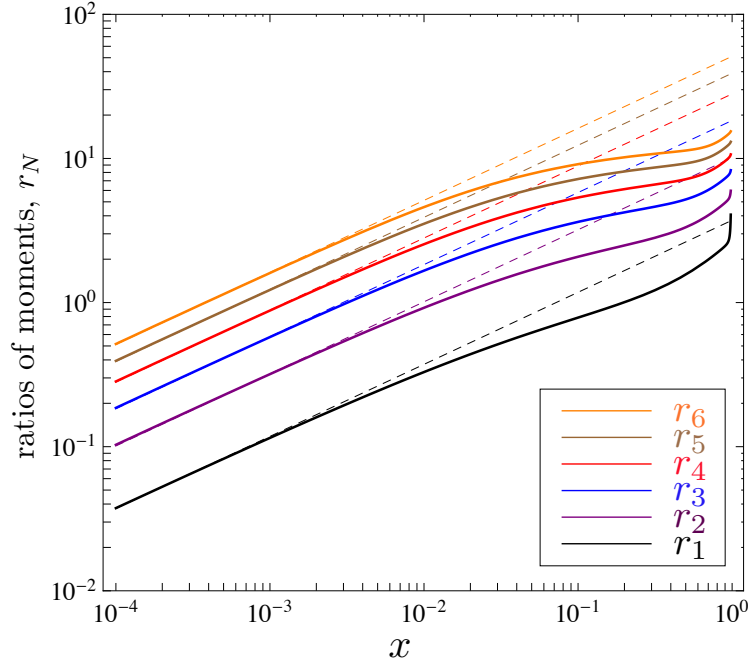


Figure A.3: (Color online.) The ratios of moments, $r_N \equiv x^2 M_N / M_{N-1}$ ($N = 1 \rightarrow 6$ from bottom to top), of the transverse momentum distribution, for the following set of parameters: $\hat{q} = 1 \text{ GeV}^2/\text{fm}$, $E = 100 \text{ GeV}$, $L = 4 \text{ fm}$, $\bar{\alpha} = 0.3$. The small- x limit extrapolations are indicated by dashed lines.

Appendix A.1. The region $x \lesssim 1$

When x is very close to 1, the angular distribution is not affected by gluon branching, and its soft component is given by the Gaussian (48), which is entirely characterized by the second moment $\langle \theta^2(x, L) \rangle = \theta_s^2(x, L)$.

Appendix A.2. The region $x_s \ll x \ll 1$

When $x_s \ll x$ gluon branching can be taken into account perturbatively. For x not too small, the distribution remains determined by the first moment

$$M_1(x, L) = \frac{\hat{q}L}{2E^2} \left(1 + \frac{1}{x^2} \right) D^{(1b)}(x, L). \quad (\text{A.4})$$

When multiplied by $x^2 E^2$ this moment represents the average momentum squared. The first contribution represents the average momentum square acquired by the gluon before its splitting, the second contribution is that acquired after the splitting. The factor 1/2 comes from the averaging over the time of the splitting in the interval $[0, L]$. Note that as x becomes small, the first contribution becomes negligible: the entire contribution to the average momentum squared comes then from momentum broadening of the observed gluon since the time of its emission. We focus now on this contribution and write the first moment as

$$M_1(x, L) = \frac{\hat{q}L}{2x^2 E^2} D^{(1b)}(x, L). \quad (\text{A.5})$$

More generally, by keeping the zero branching approximation for the Green's function in Eq. (A.3), we obtain a simple recursion relation for the moments:

$$M_N(x, L) = \frac{N^2 \hat{q}}{x^2 E^2} \int_0^L dt M_{N-1}(x, t). \quad (\text{A.6})$$

This can be solved in the form

$$M_N(t) = a_N (\theta_s^2(x, t))^N D^{(1b)}(x, L), \quad (\text{A.7})$$

where

$$\theta_s^2(x, t) \simeq \frac{\hat{q}t}{2(xE)^2} = \frac{1}{2x^2} \frac{t}{L} \theta_s^2(L). \quad (\text{A.8})$$

The recursion relation for the a_N reads

$$a_N = N^2 \left(\int_0^1 du u^N \right) a_{N-1} = \frac{N^2}{N+1} a_{N-1} = \frac{N!}{N+1}, \quad (\text{A.9})$$

so that the moments take eventually the form

$$M_N(L) = \frac{N!}{N+1} \frac{\theta_s^{2N}(L)}{x^{2N}} D^{(1b)}(x, L). \quad (\text{A.10})$$

In particular, we have

$$r_N \equiv x^2 \frac{M_N}{M_{N-1}} = \frac{N^2}{N+1} \theta_s^2 = \frac{N^2}{N+1} \frac{\hat{q}L}{E^2}. \quad (\text{A.11})$$

This ratio is independent of x , a feature that can be recognized in Fig. A.3 for the largest values of N that are plotted. The moments that we have obtained correspond to the moments of the angular distribution of the primarily emitted gluon (the BDMPSZ gluon), namely,

$$D(x, \boldsymbol{\theta}, L) = \int_0^L dt \frac{4\pi}{\theta_s^2(x, t)} \exp \left[-\frac{\boldsymbol{\theta}^2}{\theta_s^2(x, t)} \right] D^{(1b)}(x, L), \quad (\text{A.12})$$

with $D^{(1b)}(x, t) = (t/t_*)/\sqrt{x}$. It can indeed be verified that the moments of the distribution (A.12) coincide with those given in Eq. (A.7).

Appendix A.3. Small- x limit

When $x \ll x_s$ multiple branchings are important and have to be fully taken into account. By using the same reasoning as that which leads to Eq. (43), one easily obtain from Eq. (A.3)

$$M_N(x, L) = \frac{N^2 \sqrt{\hat{q}E}}{2\pi\bar{\alpha}E^2} \int_x^1 \frac{dy}{y^3} \frac{\sqrt{y}}{\sqrt{x/y}\sqrt{1-x/y}} M_{N-1}(y, L). \quad (\text{A.13})$$

This relation between moments confirms the fact that their time dependence is essentially unaltered as N increases. In fact the entire L dependence factorizes and drops in the ratio M_N/M_0 defining $\langle \theta^{2N} \rangle$ (see Eq. (A.1)). Recalling indeed that in the scaling region $x, y \ll 1$, we have $D(y, L)/D(x, L) = \sqrt{x/y}$ we obtain the L -independent recursion formula for the moments

$$\langle \theta^{2N} \rangle(x) = \frac{2N^2}{\pi} \theta_*^2(x) \int_x^1 du \sqrt{\frac{u}{1-u}} \langle \theta^{2(N-1)} \rangle(x/u), \quad (\text{A.14})$$

where $u = x/y$ and

$$\theta_*^2(x) \equiv \frac{1}{4\bar{\alpha}} \left[\frac{\hat{q}}{(xE)^3} \right]^{1/2} = \langle \theta^2 \rangle, \quad (\text{A.15})$$

is the typical angle squared of gluons in the multiple branching regime. The prefactor $1/4$ is chosen to match the first moment, i.e., $\langle \theta^2 \rangle = \theta_*^2(x)$. Note that this angle $\theta_*(x)$ is independent of the size of the medium.

In order to solve the recursion relation (A.14) we set

$$\langle \theta^{2N} \rangle = a_N \theta_*^{2N}(x). \quad (\text{A.16})$$

We then obtain the following equation for the coefficients a_N :

$$a_N = \frac{2N^2}{\pi} \int_0^1 du \frac{u^{\frac{3N-2}{2}}}{\sqrt{1-u}} a_{N-1} = \frac{2N^2}{\sqrt{\pi}} \frac{\Gamma(\frac{3N}{2})}{\Gamma(\frac{1+3N}{2})} a_{N-1}. \quad (\text{A.17})$$

The first four coefficients of the moments are,

$$a_0 = 1, \quad a_1 = 1, \quad a_2 = \frac{128}{15\pi}, \quad a_3 = \frac{42}{\pi}. \quad (\text{A.18})$$

These differ somewhat from the corresponding values $a_N = N!$ for the exponential distribution. In fact, at large N , Stirling formula ($\Gamma(x) \sim x^{-x}$) allows us to write

$$a_N \sim N^{\frac{3N}{2}} \sim \Gamma\left(\frac{3N}{2}\right). \quad (\text{A.19})$$

These values are those corresponding to a distribution that falls like $e^{-c\theta^\beta}$,

$$a_N = \int d\theta^2 \theta^{2N} e^{-c\theta^\beta} \sim \Gamma\left(\frac{2N}{\beta}\right), \quad (\text{A.20})$$

with $\beta = 4/3$. This suggests that the soft part of the angular distribution behaves at large angles as

$$D(x, \theta, L) \sim e^{-c\theta^{4/3}}. \quad (\text{A.21})$$

Of course, this asymptotic behavior is only that of the soft part of the distribution, for which moments exist. It is visible in Fig. 2, but will be hidden by that actual tail corresponding to single scatterings.

References

- [1] **Atlas** Collaboration, G. Aad *et al.*, Phys. Rev. Lett. **105** (2010) 252303.
- [2] **CMS** Collaboration, S. Chatrchyan *et al.*, Phys. Rev. **C84** (2011) 024906.
- [3] **CMS** Collaboration, S. Chatrchyan *et al.*, CMS-PAS-HIN-14-010.
- [4] **CMS** Collaboration, S. Chatrchyan *et al.*, Phys.Lett. **B712** (2012) 176.
- [5] B. Schenke, C. Gale and S. Jeon, *Phys.Rev.* **C80**, 054913 (2009), arXiv:0909.2037 [hep-ph].
- [6] K. C. Zapp, J. Stachel and U. A. Wiedemann, *JHEP* **1107**, 118 (2011), arXiv:1103.6252 [hep-ph].
- [7] T. Renk, *Phys.Rev.* **C78**, 034908 (2008), arXiv:0806.0305 [hep-ph].
- [8] N. Armesto, L. Cunqueiro and C. A. Salgado, *Eur.Phys.J.* **C63**, 679 (2009), arXiv:0907.1014 [hep-ph].
- [9] J. -P. Blaizot, F. Dominguez, E. Iancu and Y. Mehtar-Tani, arXiv:1311.5823 [hep-ph].
- [10] J. -P. Blaizot, Y. Mehtar-Tani and M. A. C. Torres, arXiv:1407.0326 [hep-ph].
- [11] A. Kurkela and U. A. Wiedemann, arXiv:1407.0293 [hep-ph].
- [12] R. Baier, Y. L. Dokshitzer, A. H. Mueller, S. Peigne, and D. Schiff, Nucl. Phys. **B483** (1997) 291; Nucl. Phys. **B484** (1997) 265.
- [13] B. G. Zakharov, JETP Lett. **63** (1996) 952.
- [14] R. Baier, A. H. Mueller, D. Schiff, and D. Son, Phys. Lett. **B502** (2001) 51.
- [15] R. Baier, Y. L. Dokshitzer, A. H. Mueller, and D. Schiff, JHEP **09** (2001) 033.
- [16] J. -P. Blaizot and Y. Mehtar-Tani, in preparation.
- [17] L. Fister and E. Iancu, arXiv:1409.2010 [hep-ph].
- [18] J. P. Blaizot, F. Dominguez, E. Iancu and Y. Mehtar-Tani, JHEP **1301** (2013) 143, arXiv:1209.4585 [hep-ph].
- [19] J. -P. Blaizot and Y. Mehtar-Tani, Nucl. Phys. **A929** (2014) 202, arXiv:1403.2323 [hep-ph].
- [20] T. Liou, A. H. Mueller and B. Wu, Nucl. Phys. **A916** (2013) 102, arXiv:1304.7677 [hep-ph].
- [21] E. Iancu, arXiv:1403.1996 [hep-ph].
- [22] J. -P. Blaizot, E. Iancu and Y. Mehtar-Tani, Phys. Rev. Lett. **111**, 052001 (2013).
- [23] J. P. Blaizot, F. Gelis and R. Venugopalan, Nucl. Phys. **A743** (2004) 13, [hep-ph/0402256].
- [24] Y. Mehtar-Tani and K. Tywoniuk, arXiv:1401.8293 [hep-ph].